Cytochrome *c* Peroxidase Mutant Active Site Structures Probed by Resonance Raman and Infrared Signatures of the CO Adducts†

Giulietta Smulevich,*,‡ J. Matthew Mauro,§ Laurence A. Fishel,§ Ann M. English,∥ Joseph Kraut,§ and Thomas G. Spiro*,⊥

Dipartimento di Chimica, Università di Firenze, Via G. Capponi 9, 50121 Firenze, Italy, Department of Chemistry, University of California, San Diego, La Jolla, California 92093, Department of Chemistry, Concordia University, Montreal, Quebec, Canada H3G 1M8, and Department of Chemistry, Princeton University, Princeton, New Jersey 08544

Received January 28, 1988; Revised Manuscript Received April 4, 1988

ABSTRACT: Vibrational frequencies associated with FeC and CO stretching and FeCO bending modes have been determined via resonance Raman (RR) and infrared (IR) spectroscopy for cytochrome *c* peroxidase (CCP) mutants prepared by site-directed mutagenesis. These include the bacterial "wild type", CCP(MI), and mutations involving groups on the proximal (Asp-235 → Asn; Trp-191 → Phe) and distal (Trp-51 → Phe; Arg-48 → Leu and Lys) side of the heme. The data were analyzed with the aid of a recently established correlation between ν_{FeC} and ν_{CO}, which can be used to distinguish between back-bonding and axial ligand donor effects. At high pH all adducts showed essentially the same vibrational pattern (form I′) with ν_{FeC} ~ 505 cm^{-1}, ν_{CO} ~ 1948 cm^{-1}, and δ_{FeCO} (weak RR band) ~ 576 cm^{-1}. These frequencies are very similar to those shown by the myoglobin CO adduct and imply a "normal" H-bond of the proximal histidine. At pH 7 (pH 6 for Asn-235 and Leu-48), different forms are seen for different proteins: form I (ν_{FeC} ~ 500 cm^{-1}, ν_{CO} = 1922–1941 cm^{-1}, and δ_{FeCO} ~ 580 cm^{-1}, very weak) in the case of CCP(MI) and Phe-191, as well as bakers' yeast CCP, or form II (ν_{FeC} ~ 530 cm^{-1}, ν_{CO} = 1922–1933 cm^{-1}, and δ_{FeCO} = 585 cm^{-1}, moderately strong) for Asn-235 and Phe-51. Both forms are seen for Phe-191 and bakers' yeast CCP; low CO pressures favor form I while form II grows at 1 atm of CO pressure, implying that a second CO molecule is bound. The ν_{FeC} and ν_{CO} values indicate that the H-bond from the proximal His-175 to the nearby Asp-235 is maintained in form I adducts of Arg-48-containing proteins but is weakened in the Leu-48 and Lys-48 form I adducts. The strong proximal H-bond is also lost or weakened in all form II adducts. It is proposed that CO binding places the His-175–Asp-235 interaction under tension, which is maintained by anchoring the polypeptide chain near the proximal His-175 with a H-bond from His-181 to a heme propionate group; this group is oriented by another H-bond, from a water molecule which is H-bonded to Arg-48. Replacement of Arg-48, or deprotonation of His-181 (in form I′), loosens this anchor and allows disruption of the His-175–Asp-235 H-bond. The form II adducts have ν_{FeC} and ν_{CO} values indicating extra Fe → CO back-donation, attributable to strong distal H-bonding of the bound CO. The H-bond donor is proposed to be Arg-48 whose disposition (H-bonded to the Fe-bound CO or H-bonded to the heme propionate bound H_2O) is suggested to be coupled to protonation of the distal His-52 residue and to binding of a second CO molecule. The reorientation of the Arg-48 and the distal H-bond formation then explain the disruption of the proximal His-175–Asp-235 H-bond in form II. Photoinstability of the CO adducts increases in the order form I′ < form II < form I, implying a reverse order for the CO recombination rates. A lower recombination rate for form II is attributed to the requirement for distal H-bond formation, while the still lower rate for form I is attributed to the tension on the proximal His-175–Asp-235 H-bond.

The vibrational spectrum of the carbon monoxide adduct of heme proteins (Tsubaki et al., 1982) is a useful probe for interactions of the heme group with protein residues in the heme pocket. In the preceding paper (Smulevich et al., 1988) the heme environment of cytochrome *c* peroxidase (CCP) has been investigated by monitoring the ligation state of mutants in which residues capable of interacting with the heme group via its ligands on both the proximal and distal sides were replaced. In the present study we continue this investigation by using the vibrational signatures of the CO adducts as probes of the heme environment. The CO stretching frequency is readily determined from the infrared spectrum of the protein. The FeC stretching vibration is seen as a moderately strong band in the Soret-excited resonance Raman spectrum (RR); a RR band corresponding to the FeCO bending vibration can sometimes also be seen. These modes are readily identified via their characteristic ^{13}CO and $C^{18}O$ frequency shifts (Tsubaki et al., 1982).

Vibrational data have now been collected on numerous heme CO adducts, and a number of regularities have been noted (Kerr & Yu, 1987; Uno et al., 1987; Li & Spiro, 1988). Principal among these is a negative correlation between ν_{FeC} and ν_{CO} due to the Fe → CO π-back-donation which dominates the bonding in these species. In a previous study of CO adducts of bakers' yeast CCP (Smulevich et al., 1986) and HRP (Evangelista-Kirkup et al., 1986), we found a CO pressure dependent conformational equilibrium between two forms, one of which showed unusually strong back-donation, with elevated ν_{FeC} and depressed ν_{CO}, associated with a distal H-bond to the

† Supported by NIH Grant GM 33576 (to T.G.S.), NATO Grant 86/0453 (to G.S., A.M.E., and T.G.S.), NSF Grant DMB-8511656 (to J.K.), and NRSA Postdoctoral Fellowship PHS GM 10292-02 (to J.M.M.).

* Authors to whom correspondence should be addressed.
‡ Università di Firenze.
§ University of California, San Diego.
∥ Concordia University.
⊥ Princeton University.

0006-2960/88/0427-5486$01.50/0

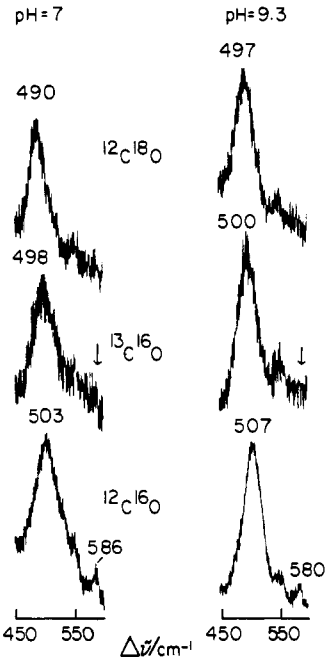

FIGURE 1: Resonance Raman spectra of CCP(MI)–CO and its ^{13}CO and $C^{18}O$ analogues at different pHs. The arrows indicate the disappearance of the δ_{FeCO} bending mode in the ^{13}CO adduct. Experimental conditions: laser power, ~ 5 mW at the sample; spectral slit width, 5 cm^{-1}; accumulation time, 5 s/0.5 cm^{-1}.

bound CO. The mutant proteins examined in this study show strong variations with regard to the mode of CO binding which clarify the sources of this unusual conformational equilibrium and further illuminate the interaction of the heme group with its protein surroundings.

Experimental Procedures

CCP(MI) and its mutants were expressed in *Escherichia coli* as previously described (Fishel et al., 1987; Smulevich et al., 1988). Crystals of the proteins were dissolved in 0.1 M phosphate (pH 6–7) and Tris-HCl (pH 8.5–9.3) buffers to give a protein concentration of 0.3–0.5 mM for RR spectroscopy and 1.5–2.5 mM for IR spectroscopy. The CO adducts were obtained by gently flowing CO (1 atm) (Matheson) over the surface of the reduced protein (obtained by adding a minimum volume of sodium dithionite) for 20 min. The ^{13}CO (99%) and $C^{18}O$ (98%) adducts were obtained by introducing the gas (Cambridge Isotope Labs) from 0.25- and 0.1-L glass flasks, respectively, to an evacuated NMR tube.

Resonance Raman spectra were obtained with excitation from the 413.1-nm line of a Kr^+ laser (Spectra Physics 171) according to procedures described in the preceding paper (Smulevich et al., 1988). The spectra were obtained at room temperature at low laser power (~5 mW). Under these conditions, photolysis was negligible, as could be determined from the intensity ratio of the ν_4 porphyrin bands associated with the ligated and deligated forms. Infrared spectra were recorded at 25 °C with a DIGILAB FDS-20C FTIR spectrophotometer. The samples were transferred by a syringe flushed with CO to a CaF_2 IR cell (0.1-mm path length) which has been flushed with CO. Buffer solution was used as a reference. The CaF_2 windows permitted UV/vis absorption spectra to be recorded immediately before and after IR spectroscopy.

Results

Figures 1–5 show fragments of the CO adduct RR spectra of the CCP mutants included in this study, in the region of the Fe–C stretching and Fe–C–O bending frequencies, while Figure 6 shows IR spectra in the region of the C–O stretch. The C–O stretching band stands out clearly in the IR spectra and shows characteristic shifts between high- and low-pH forms of the proteins. The RR bands are identified via ^{13}CO and $C^{18}O$ isotope shifts, as illustrated in the figures. The Fe–C stretching frequency, ν_{FeC}, shifts down by ~6 and ~12 cm^{-1} for the ^{13}CO and $C^{18}O$ adducts, respectively, while the Fe–C–O bending frequency, δ_{FeCO}, is expected to show a characteristic "zigzag" pattern with ~16- and ~0-cm^{-1} shifts for ^{13}CO and $C^{18}O$, respectively (Tsubaki et al., 1982). The δ_{FeCO} mode is quite weak in most of the spectra, although an intensity loss for a band near 580 cm^{-1} can frequently be seen upon ^{13}CO substitution. Relatively strong δ_{FeCO} bands are seen only for Phe-191, Asn-235, and Phe-51 mutants at low pH (Figures 2–4).

The frequencies can be arranged into three distinct patterns, as shown in Table I, corresponding to three kinds of CO ad-

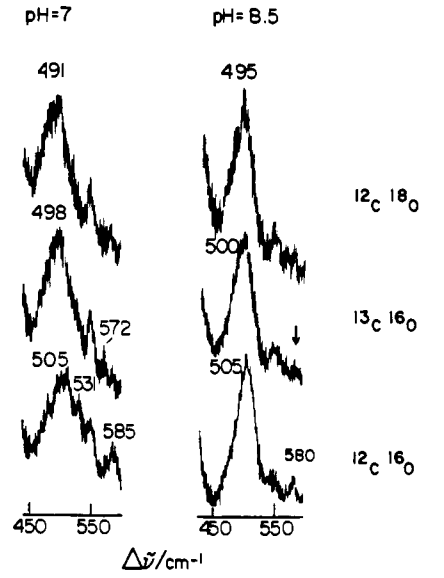

FIGURE 2: RR spectra of CCP(MI-Phe-191)–CO and its ^{13}CO and $C^{18}O$ analogues at different pHs. The arrows indicate the disappearance of the δ_{FeCO} bending mode in the ^{13}CO adduct. Experimental conditions as Figure 1.

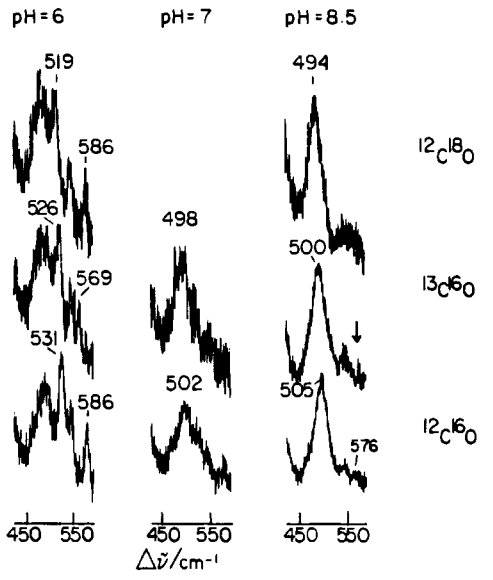

FIGURE 3: RR spectra of CCP(MI-Asn-235)–CO and its ^{13}CO and $C^{18}O$ analogues at different pHs. The arrows indicate the disappearance of the δ_{FeCO} bending mode in the ^{13}CO adduct. Same conditions as Figure 1.

Table I: FeCO Vibrational Frequencies and Isotope Shifts (cm^{-1}) for CCP Mutants

	high-pH form I′			low pH					
				form I			form II		
	ν_{FeC}	δ_{FeCO}	ν_{CO}	ν_{FeC}	δ_{FeCO}	ν_{CO}	ν_{FeC}	δ_{FeCO}	ν_{CO}
CCP[a]	503	575	1948	495		1922	530	585	1922
CCP(MI)	507 (7, 10)[b]	580	1948	503 (5, 13)	586	1922			
Phe-191	505 (5, 10)	580	1950	505 (7, 14)		1922	531	~585	[c]
Asn-235	505 (5, 11)	576	1951				531 (5, 12)	586 (17)	1933
Phe-51	505 (5, 10)	~580	1948				528 (5, 10)	585 (16)	1932
Leu-48	500 (4, 9)	580	1951	500	582	1941			
Lys-48	507 (5, 10)	~580	1945	510 (6, 13)	586	1936			

[a] From Smulevich et al. (1986). [b] Isotope shifts ($\Delta^{13}CO$, $\Delta C^{18}O$). [c] It proved impossible to measure the ν_{CO} IR band at the high CO pressure required for Phe-191 form II formation.

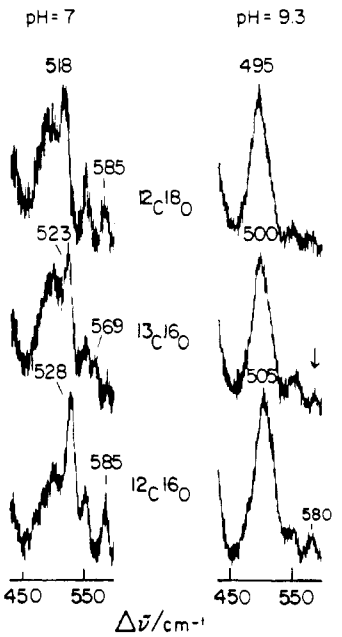

FIGURE 4: RR spectra of CCP(MI-Phe-51)–CO and its ^{13}CO and $C^{18}O$ analogues at different pHs. The arrows indicate the disappearance of the δ_{FeCO} bending mode in the ^{13}CO adduct. Same conditions as Figure 1.

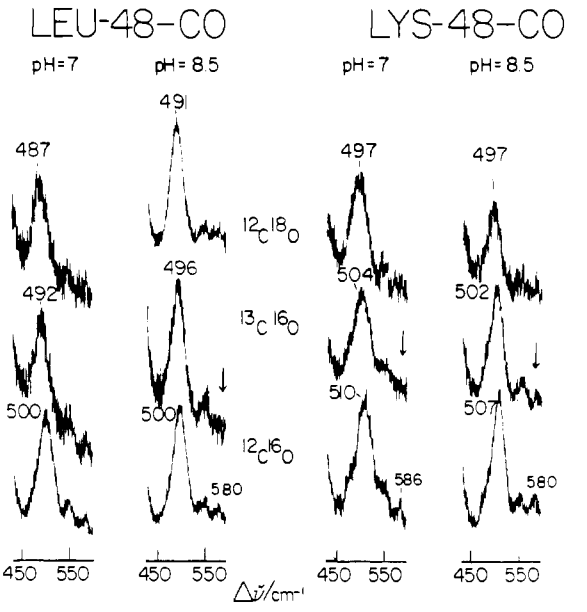

FIGURE 5: RR spectra of CCP(MI-LeuH48)–CO and CCP(MI-Lys-48)–CO and its ^{13}CO and $C^{18}O$ analogues at different pHs. The arrows indicate the disappearance of the δ_{FeCO} bending mode in the ^{13}CO adduct. Same conditions as Figure 1.

ducts, which we label forms I′, I, and II [form I′ was called form II′ in Smulevich et al. (1986) but has been relabeled here to emphasize the greater simularity with form I]. Form I′ is a common structure shown by all of the proteins at high pH. It has ν_{CO} = 1945–1951 cm^{-1}, ν_{FeC} = 503–507 cm^{-1}, and δ_{FeCO} = 575–580 cm^{-1}, although the last mode appears only weakly in the RR spectra. The frequencies are in the cited narrow ranges except that the Leu-48 mutant shows a slightly depressed ν_{FeC}, at 500 cm^{-1}.

Forms I and II are found at low pH, and their spectra exhibit considerable variation. Form I shows ν_{FeC} in the 500-cm^{-1} region, although the range is 495–510 cm^{-1}. δ_{FeCO} is very weak; it can only be seen for CCP(MI) (Figure 1) and for the Lys-48 (Figure 5) mutant. ν_{CO} is found at 1922 cm^{-1}, except in Leu-48 and Lys-48, where it increases markedly to 1941 and 1936 cm^{-1}, respectively. Form II shows ν_{FeC} at a high value, ~530 cm^{-1}, and a moderately strong δ_{FeCO} at 585 cm^{-1}, with ν_{CO} at 1922–1933 cm^{-1}.

It was discovered in studies of bakers' yeast CCP (Smulevich et al., 1986) and also of HRP (Evangelista-Kirkup et al., 1986) that form I converts to form II with increasing CO/protein concentration ratio. Form II is favored at high CO pressures (i.e., 20-min flushing with tank CO, at 1 atm pressure) or low protein concentrations, while form I is favored at low CO pressure (i.e., exposure from a bulb, as required in isotope experiments) or high protein concentrations. Thus, form II may involve binding of a second CO molecule, somewhere in the heme vicinity, which alters the structure of the Fe-bound CO. This behavior was also observed in the present study for the proximal Phe-191 mutant. Its 531-cm^{-1} band (Figure 2) only appears at CO tank pressure (bottom spectrum) and not when a CO bulb is used (top spectra). No form II is seen for CCP(MI) (Figure 1), which differs in this respect from bakers' yeast CCP (Smulevich et al., 1986). Nor is form II seen for the Leu-48 or Lys-48 mutants (Figure 5). On the other hand, only form II is observed for the Asp-235 (figure 3) and Phe-51 (Figure 4) mutants. The presence of a small amount of form I cannot, however, be excluded because of interferences from a porphyrin band at ~495 cm^{-1}. We infer that the secondary binding of CO that is needed to convert form I to form II does not occur, or is too weak for form II detection at 1 atm of CO pressure, in the case of (CCP(MI) and of the Leu-48 and Lys-48 mutants. On the other hand, for the Asn-235 or Phe-51 mutants secondary CO binding is not required for form II formation, or it is sufficiently strong that even low CO concentrations are sufficient for essentially complete conversion to form II. The CO-dependent equilibrium between forms I and II is manifested only by the Phe-191 mutant or by bakers' yeast CCP.

The transition pH for the conversions of forms I and II to form I′ varies somewhat with the protein. It lies between 7 and 8.5 for the Lys-48 and Phe-191 mutants since the form I′ vibrational bands are absent at pH 7 and fully grown in at

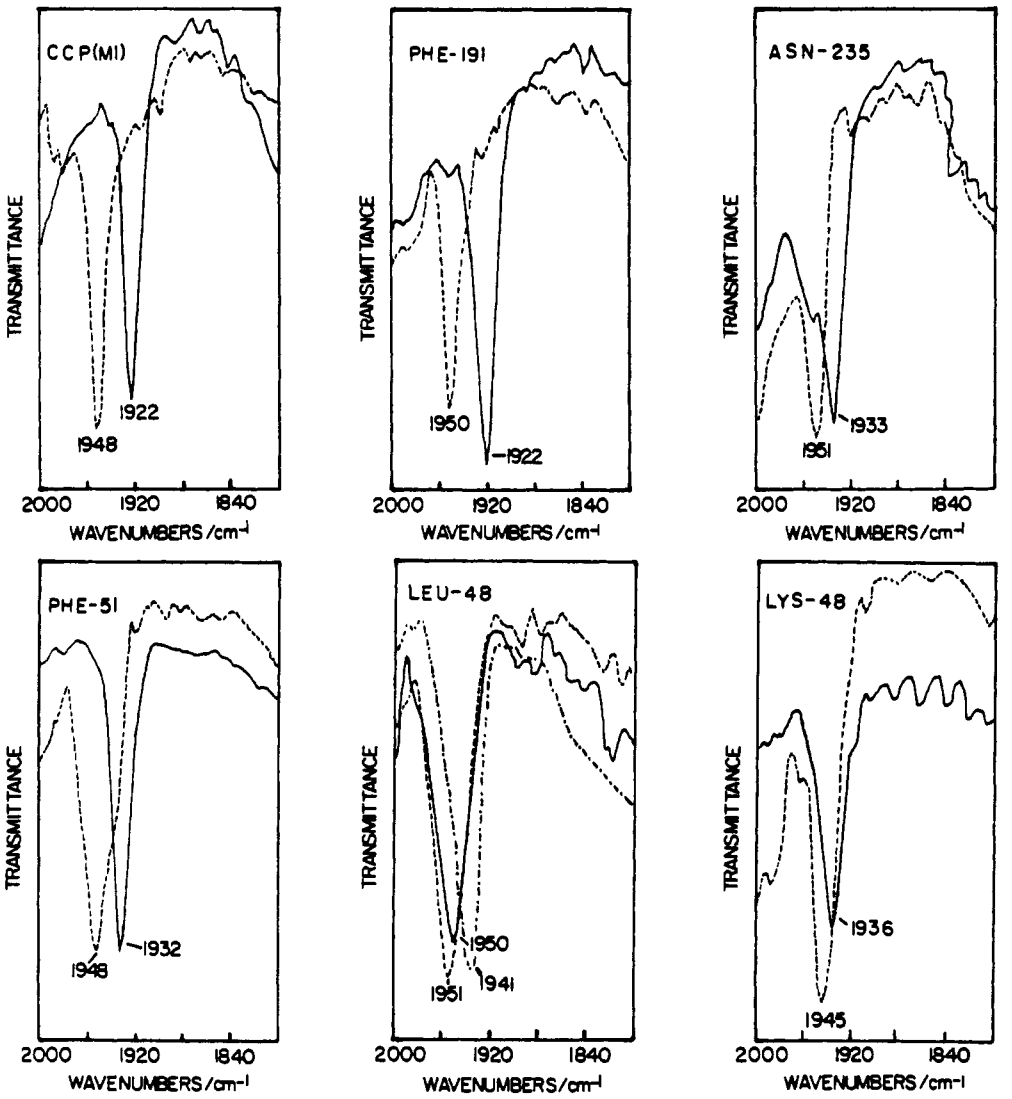

FIGURE 6: IR spectra of the CO adducts of the six mutants at different pHs: (···) pH 6 (Leu-48 only); (—) pH 7; (– –) pH 8.5. Accumulation time, 128 transients; spectral resolution, 8 cm^{-1}.

pH 8.5. For CCP(MI) and the Phe-51 mutant, however, the transition pH is >8.5 since the pH had to be raised to pH 9.3 to completely suppress the form I and II RR bands. The transition is near pH 7 for the Asn-235 mutant as evidenced by the form I′ contributions [1953-cm^{-1} IR shoulder (Figure 6) and the 502-cm^{-1} RR band (Figure 3)] even at neutral pH. For the Leu-48 mutant the transition occurs between pH 6 and 7 (Figure 6).

Discussion

Interpretation of the data is facilitated by correlating the ν_{FeC} and ν_{CO} frequencies as shown in Figure 7. It has been found (Kerr & Yu, 1987; Uno et al., 1987; Li & Spiro, 1987) that the data for numerous heme CO adducts fall on a single straight line, the one shown in the figure. The negative slope is expected from the back-donation model of FeCO bonding, in which donation of Fe d_π electrons into the CO π^* antibonding orbitals lowers the C–O bond strength while raising the Fe–C bond strength. The extent of back-donation can be increased by increasing the electron density at Fe, e.g., with electron-donating substituents on the porphyrin, or by increasing the donor strength of the trans axial ligand, or it can be increased by polarization of the O atom of the bound CO by positive charges or H-bonding (Li & Spiro, 1987). Increasing back-donation moves a point upward along the line.

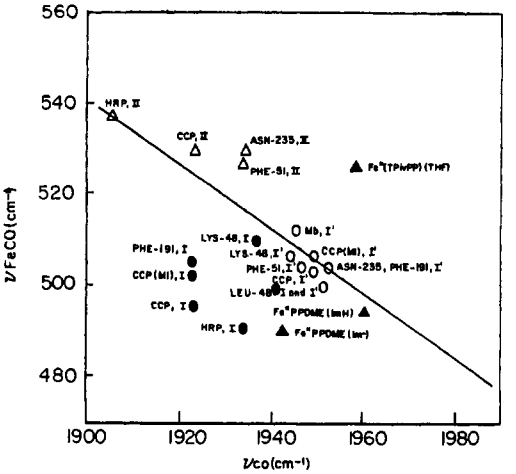

FIGURE 7: Plot of observed ν_{FeCO} vs ν_{CO} adducts of the six mutants, together with Hb, CCP, HRP, and analogue complexes. The line represents a least-squares fit for a large number of heme CO adducts with imidazole ligands.

When the axial ligand donation is increased, however, an additional effect is superimposed on back-donation. The Fe–CO bond strength is decreased, due to competition for the σ bonding orbital d_z^2, without a compensating increase in the C–O strength. Thus heme CO adducts with strong donor axial

ligands fall below the line of Figure 7 while those with weak donor axial ligands fall above the line (Li & Spiro, 1987). The examples which fall on the line have imidazole as proximal ligand. The dependence on the axial ligand is illustrated by three model compounds, (CO)Fe^{II}PPDME(ImH) (PPDME = protoporphyrin IX dimethyl ester, ImH = imidazole), (CO)Fe^{II}PPDME(Im^-), and (CO)Fe^{II}(TPivPP)(THF) (TPivPP = mesotetrakis[(pivaloylamido)phenyl)]porphine, THF = tetrahydrofuran), shown as filled triangles in Figure 7. The imidazole complex falls close to the line, but when the imidazole is deprotonated, the point falls well below the line, due to the stronger σ donating ability of imidazolate (Evangelista-Kirkup et al., 1986). THF is a very weak ligand, and the point for the THF complex falls far above the line (Kerr & Yu, 1987).

Increased σ donation from the axial ligand also decreases ν_{CO}. Thus (CO)Fe^{II}PPDME(Im^-) has a substantially lower ν_{CO} than (CO)Fe^{II}PPDME(ImH). This is because deprotonation of the imidazole raises the electron density on the Fe, thereby increasing the back-donation to the CO; there may also be a contribution from direct overlap of the filled imidazole π orbitals (π donation) with the Fe d_π orbitals responsible for back-donation. Conceptually, the vertical distance to the line in Figure 7 gives the σ competition effect (on ν_{FeC}) while the horizontal distance gives the back-donation effect (on ν_{CO}); both effects are relative to a "standard" imidazole ligand.

But there are also distal influences on back-donation; polar groups in the vicinity of the bound CO can be expected to modulate the drift of electrons from the Fe d_π to the CO π^* orbitals. The largest polarization effect, giving the highest points on the Figure 7 line, is associated with H-bonding to the carbonyl O atom (vide infra). But other distal polar effects no doubt account for the dispersion of the points along the line. Thus the myoglobin CO adduct shows substantially greater back-donation than the (CO)Fe^{II}PPDME(ImH) model compound (Figure 7), probably because the bound CO abuts a distal histidine residue. Although no H-bond is formed (Kuriyan et al., 1986), a polarization effect is likely. In addition the interaction prevents the CO from adopting its normal orientation, perpendicular to the heme. The resulting distortion, probably involving a tilt of the Fe–C–O linkage relative to the heme plane (Kerr et al., 1983; Li & Spiro, 1988), may also contribute to increased back-donation (due to decreased competition from the porphyrin π^* acceptor orbitals; Li & Spiro, 1988). Thus there may be multiple distal influences on the extent of back-donation.

Forms I and I′: Arg-48 and His-181 Anchor the Proximal H-Bond. When the present CCP data are plotted on the ν_{FeC}, ν_{CO} correlation (Figure 7), several groupings emerge. All of the form I′ complexes fall close to the line in a narrow region near the point representing the CO complex of myoglobin (Tsubaki et al., 1982). Thus these alkaline complexes all show behavior expected of CO adducts with a standard imidazole ligand. In contrast, most of the low-pH form I adducts, those of CCP(MI) and the Phe-191 mutant, as well as bakers' yeast CCP and also HRP, fall well below the line. This behavior is consistent with substantial imidazolate character of the CCP (and HRP) proximal ligand. In the ligand-free Fe^{II} species as well, proximal imidazolate character is evident in the high frequency, $\sim$240 cm^{-1}, of the Fe–His stretching mode and is attributed to a strong H-bond from the proximal His-175 to the carboxylate side chain of Asp-235 (Smulevich et al., 1988). It can therefore be inferred that conversion of the CO adducts from form I to form I′ at alkaline pH must involve a switch from imidazolate to imidazole character via a weakening of the His-175–Asp-235 interaction. The ligand-free Fe^{II} species likewise gives evidence that high pH diminishes the imidazolate character of the proximal ligand (Smulevich et al., 1988). But in the Lys-48 and Leu-48 CO adducts, some disruption of the His-175–Asp-235 interaction is inferred *even at low pH*, since the form I points for these mutants fall closer to the line, than the other form I species.

We offer a structural interpretation of these findings involving H-bonding interactions in the heme pocket, consistent with the results of the preceding study (Smulevich et al., 1988). The structure of bakers' yeast CCP (Finzel et al., 1984; see Figure 14 of the preceding paper) shows two titratable histidine residues in the vicinity of the heme, His-52 and His-181. (The third His residue in the region, His-175, is bound to the Fe atom and is therefore not protonatable.) It is notable that the pH dependencies of the Soret band wavelength of the bakers' yeast CCP CO adduct, and also of its CO recombination rate, are governed by a *two-proton* dissociation (Iizuka et al., 1985) with a pK_a of 7.5. We suggest that the two titratable protons reside on His-52 and His-181. His-181, which is separated by only five residues from the proximal His-175, donates a H-bond to a heme propionate anion. Deprotonation of His-181 would destroy this anchoring interaction. The resulting flexibility of the proximal chain connecting His-175 with His-181 could account for the weakening of the His-175–Asp-235 interactions at high pH, which is indicated for the CO adducts as well as for the ligand-free proteins.

In addition to His-181, the distal Arg-48 residue is an important determinant of the state of the proximal linkage, in view of the inferred weakening of the His-175–Asp-235 interaction in the Leu-48 and Lys-48 mutants upon CO binding, even at low pH. The Arg-48 side chain is H-bonded to a water molecule, which in turn donates a H-bond to the same heme propionate group that anchors the His-181 residue. It is plausible that the Arg-48 interaction fixes the orientation of the propionate residue, which may otherwise be free to take up alternative conformations via rotations about the three single bonds in the propionate chain. This freedom might allow the proximal chain between His-175 and His-181 enough flexibility to weaken the His-175–Asp-235 interaction upon CO binding, even if the His-181 propionate H-bond is maintained. At low pH the ligand-free Fe^{II} forms of the Leu-48 and Lys-48 mutants do maintain a strong His-175–Asp-235 interaction (Smulevich et al., 1988), evidenced by the $\sim$ 240-cm^{-1} Fe-His vibration. The weakening of this interaction in the low-pH CO adducts is attributable to the displacement of the Fe atom toward the heme plane upon binding a sixth, distal ligand. Thus CO binding to the Leu-48 and Lys-48 mutants throws a switch between two proximal conformations, one with and the other without a strong His-175–Asp-235 interaction.

But this switch is *not* thrown in the form I adducts of the Arg-48-containing proteins. We conclude that the Arg-48–H_2O–propionate–His-181 H-bond system anchors the proximal chain sufficiently to inhibit disruption of the His-175–Asp-235 linkage even when CO is bound. This linkage must be under some strain, however, as can be inferred by the fact that the points for the form I adducts show appreciable scatter in Figure 7, deviating from the line by different amounts. The strain is enough to disrupt the linkage when His-181 is deprotonated (form I′ adducts) or when Arg-48 is missing (Leu-48 and Lys-48 adducts at low and high pH).

Form II: H-Bonding to CO from Arg-48. The conformational switch *is* thrown for the form II adducts, all of which fall on or above the line in Figure 7, implying a disrupted

His-175–Asp-235 linkage. In addition, these adducts are at the high end of the correlation, indicating unusually extensive back-donation. The extra back-donation is attributable to a distal H-bond to the O atom of the bound CO, which has the effect of polarizing the π^* orbitals and inducing a stronger migration of electrons from the Fe. This H-bond has been demonstrated experimentally by the measurable D_2O shifts seen for the form II ν_{CO} IR bands of HRP (Smith et al., 1983) and CCP (Satterlee et al., 1984). We note (Figure 7) that the ν_{CO} frequencies are as low or lower in the form I as in the form II adducts (except for HRP), but much of this lowering is attributable to the enhanced donor character of the proximal ligand, as discussed above in connection with the model complexes. If the ν_{CO} difference between (CO)Fe^{II}PPDME(Im^-) (CO)Fe^{II}PPDME(ImH) is taken as a guide, then correction for the donor effect would place the form I adducts in the same region of Figure 7 as the form I′ adducts, indicating the absence of a distal H-bond interaction for form I.

The donor group for this distal H-bond in form II has been suggested (Smulevich et al., 1986) to be the distal histidine, since form II is titrated away at pH values above neutrality. However, Arg-48 may be a better candidate since form II is not seen when Arg-48 is replaced by either Lys or Leu.

The Arg-48 side chain is conformationally flexible. In the bakers' yeast CCP Fe^{III} fluoride adduct it swings toward the Fe and H-bonds to the bound fluoride (Edwards et al., 1984). Similar H-bonding has been invoked (Smulevich et al., 1988) to explain the stabilization of a bound water molecule at low pH in Arg-48-containing proteins, and the Arg-48 movement was suggested to be triggered by the protonation of the distal His-52. The same movement could bring the Arg-48 side chain into H-bonding interaction with the bound CO. The loss of the His-175–Asp-235 proximal interaction would then be attributable to the disruption of the Arg-48–H_2O–propionate–His-181 H-bonding network discussed in the preceding section and also to the extra pull exerted on the Fe atom by the distal H-bond.

Protonation of His-52 is apparently not by itself sufficient to induce the Arg-48 movement in the CO adducts since the form I → form II conversion at low pH is induced by an increase in CO pressure, at least in the case of HRP (Evangelista-Kirkup et al., 1986), bakers' yeast CCP (Smulevich et al., 1986), and the Phe-191 mutant of CCP(MI) (present work—the point for Phe-191 form II does not appear in Figure 7 since it proved impossible to measure the ν_{CO} IR band at high CO pressure). Binding of a second CO molecule to the protein seems to be required. Where this second CO binds is presently unclear. Perhaps it displaces the water molecule through which the Arg-48 side chain interacts with the heme propionate, thereby freeing Arg-48 to form the distal H-bond. The difference between the Fe^{II} CO adduct and the Fe^{III} F^- or H_2O adduct in respect to the requirements for Arg-48 distal H-bonding may lie in the different H-bond acceptor propensity of F^- and H_2O on the one hand and CO on the other. CO is expected to be a weaker Bronsted base, even when bound to Fe^{II}. Consequently, while the energy of the distal H-bond to bound F^- or H_2O is sufficient to induce the Arg-48 side chain to leave its mooring to the propionate group, once His-52 is protonated, an extra increment of energy may be required in the case of the CO adduct. This extra increment seems to be provided by the second CO molecule.

Variation in this extra increment of energy could explain the very different propensity for form II formation among the CCP mutants, if the affinity for the second CO molecule varies reciprocally with the energy requirement (as it would, for example, if the Arg-48-anchoring H_2O molecule were being replaced). Thus form II adduct formation is facile in the Asn-235 mutant since there is no proximal His-175–Asp-235 interaction to restrain the Fe from moving to a position where the distal H-bonding is allowed. This restraint remains present in the Phe-191 mutant, but loss of the additional Asp-235–Trp-191 interaction allows limited mobility to the Fe atom, and in this case CO pressure dependent formation of form II is seen. In the parent CCP(MI), the full His-175–Asp-235–Trp-191 anchoring effect is expressed, and form II is not seen, even at 1 atm of CO pressure. Interestingly however, form II does appear at high CO pressure in bakers' yeast CCP (Smulevich et al., 1986). The sequence differences between bakers' yeast CCP and CCP(MI), Asp-153 → Gly, and Thr-53 → Ile have no obvious connection with the heme group or any of the critical heme-linked residues. We can only surmise that the heme pocket flexibility is somehow greater in bakers' yeast CCP than in CCP(MI) and that the energy requirement for form II is thereby lowered. Another surprise is the dominance of form II in the Phe-51 mutant. Here the replacement is of the Trp-51 indole side chain, which H-bonds to a water molecule positioned above the heme Fe in the Fe^{III} crystal structure (Finzel et al., 1984). Perhaps this water molecule inhibits distal H-bonding to the bound CO.

An additional point of interest is the rather large positive deviation from the line in Figure 7 seen for the Asn-235 form II adduct. This deviation implies an unusually weak donor interaction for the proximal imidazole ligand and is entirely consistent with the very low Fe–His frequency, 205 cm^{-1}, as seen for the ligand-free Fe^{II} protein (Smulevich et al., 1988). This weakness was attributed to the absence of any proximal H-bonding in the Asn-235 mutant. We note that similar behavior is seen for the heme a_3 site of cytochrome *c* oxidase, which shows a low Fe–His frequency, 210 cm^{-1}, in the ligand-free Fe^{II} form (Ogura et al., 1983) and a large positive deviation of its CO adduct from the Figure 7 line (Argade et al., 1984; Li & Spiro, 1988). It seems likely that heme a_3 also has a proximal imidazole ligand with a weak or absent H-bond.

Geometry of the FeCO Unit. Form II complexes show a relatively strong δ_{FeCO} RR band at 585 cm^{-1} and were suggested (Evangelista-Kirkup et al., 1986; Smulevich et al., 1986) to have a tilted structure. Yu and co-workers observed δ_{FeCO} in myoglobin (Tsubaki et al., 1984) and in sterically constrained protein-free heme adducts (Kerr et al., 1983) but not in unconstrained adducts. They proposed that δ_{FeCO} activation results from bending or tilting of the FeCO group. Off-axis binding of CO has been observed in crystal structures of Mb (Kuriyan et al., 1986) and other heme proteins and is attributable to steric hindrance from distal residues.

The relationship between δ_{FeCO} intensity and the FeCO geometry is not straightforward, however, as has recently been discussed (Li & Spiro, 1987). Activation of this mode requires a reduction in the fourfold electronic symmetry of the heme CO adduct, which could result from asymmetric electrostatic interactions with the protein, as well as from FeCO bending and tilting. If the strong H-bond to the bound CO in the form II adducts is at an angle with respect to the heme normal, this might account for a relatively strong δ_{FeCO} mode with or without significant off-axis distortion of the FeCO unit.

From the small frequency separation between ν_{FeCO} (530 cm^{-1}) and δ_{FeCO} (585 cm^{-1}), it can be concluded that the Fe–C–O angle does not differ substantially from 180° (Li & Spiro, 1987). Tilting of the FeCO unit relative to the heme plane is a viable distortion coordinate, however, as is buckling of the porphyrin ring (Li & Spiro, 1987). While the vibra-

tional data are not inconsistent with these distortion modes, neither do they require a distortion. Consequently, we are unable to reach any conclusions about the heme CO geometry beyond specifying that the FeCO unit is probably linear.

Photolysis. Finally, we note an interesting trend in photoinstability among the different CO adducts. The alkaline form I′ adducts are all fairly stable in the laser beam, while on the acid side the form II adducts are distinctly less stable and the form I adducts show the lowest stability. An exception to this trend is the Phe-191 form I, which is quite stable. Since the primary quantum yield for Fe–CO bond photolysis is unlikely to be influenced by the various protein interactions, we attribute the photostability variations to changes in the recombination rates. These rates are judged qualitatively to be in the order form I′ > form II > form I. The slowing of recombination in form II may be associated with the need to form a distal H-bond, which introduces an adverse entropic factor. The still greater slowing in form I is suggested to be associated with the His-175–Asp-235 H-bond, since this interaction is broken in form II but remains intact, or nearly so, in form I. The proximal H-bond is expected to inhibit movement of the Fe atom into the heme plane, which is required for CO binding. Thus, there is a straightforward structural basis for the low recombination rate and reduced photostability of the form I adducts. In the case of the Phe-191 form I, the enhanced photostability is attributable to the loss of the anchoring Trp-191–Asp-235 H-bond. The entire Fe–His-175 moiety is free to move toward the heme plane. The same reasoning would apply to the Asn-235 form I, but this species has not been detected, since form II is dominant for this mutant.

Conclusions

The RR and infrared signatures of heme-bound CO give valuable insight into the nature of heme-protein interactions in CCP, complementing those obtained in the preceding study from RR spectra of the uncomplexed reduced and oxidized forms (Smulevich et al., 1988). The effect of the strong H-bond between the proximal His-175 ligand and the nearby Asp-235 carboxylate group is expressed in the low ν_{FeC} frequency of the form I complexes which is attributable to the imidazolate character of the ligand. In this situation the heme Fe is under tension between the proximal H-bond system, which pulls it toward the proximal side, and distal forces favoring CO binding, which pull it into the plane. Consequences of this tension include the enhanced photoinstability of the form I adducts and the weakening of the His-175–Asp-235 H-bond in the Leu-48 and Lys-48 form I adducts. Maintenance of the form I strong proximal H-bond is suggested to require anchoring of the polypeptide chain near the proximal ligand via the Arg-48–H_2O–heme propionate–His-181 H-bond chain. This anchoring is lost upon replacement of Arg-48, or by deprotonation of His-181 at high pH, all form I′ adducts having a "normal" imidazole donor ligand. The proximal H-bond is disrupted in the form II adducts, which have strong distal H-bonds to the bound CO. These H-bonds are ascribed to the Arg-48 side chain, whose disposition is suggested to be coupled to protonation of His-52 and also to the binding of a second CO molecule, possibly in place of the H_2O molecule that ordinarily moors Arg-48 to the heme propionate group.

Acknowledgments

We thank Dr. Mark Miller for suggesting the importance of His-181 to the interpretation of our results.

Registry No. CCP, 9029-53-2; Asp, 56-84-8; Asn, 70-47-3; Trp, 73-22-3; Phe, 63-91-2; Arg, 74-79-3; Leu, 61-90-5; Lys, 56-87-1.

References

Argade, P. V., Ching, Y. C., & Rousseau, D. L. (1984) *Science (Washington, D.C.) 225*, 329.

Edwards, S. L., Poulos, T. L., & Kraut, J. (1984) *J. Biol. Chem. 259*, 12984.

Evangelista-Kirkup, R., Smulevich, G., & Spiro, T. G. (1986) *Biochemistry 25*, 4420.

Finzel, B. C., Poulos, T. L., & Kraut, J. (1984) *J. Biol. Chem. 259*, 13027.

Fishel, L. A., Villafranca, J. E., Mauro, J. M., & Kraut, J. (1987) *Biochemistry 26*, 351.

Gersonde, K., Kerr, E., Yu, N.-T., Parish, D. W., & Smith, K. M. (1986) *J. Biol. Chem. 261*, 8678.

Hashimoto, S., Teraoka, J., Inubushi, T., Yonetani, T., & Kitagawa, T. (1986) *J. Biol. Chem. 261*, 11110.

Iizuka, T., Makino, R., Ishimura, Y., & Yonetani, T. (1985) *J. Biol. Chem. 260*, 1407.

Kerr, E. A., & Yu, N-T. (1988) *Biological Applications of Raman Spectroscopy* (Spiro, T. G., Ed.) Vol. III, Chapter 2, Wiley-Interscience, New York.

Kerr, E. A., Mackin, H. C., & Yu, N.-T. (1983) *Biochemistry 22*, 4373.

Kuriyan, J., Wiltz, S., Karplus, M., & Petsko, G. (1986) *J. Mol. Biol. 192*, 133.

Li, X.-Y., & Spiro, T. G. (1988) *J. Am. Chem. Soc.* (in press).

Ogura, T., Hou-nami, K., Okima, T., Yoshikawa, S., & Kitagawa, T. (1983) *J. Am. Chem. Soc. 105*, 7781.

Satterlee, I. D., & Erman, J. E. (1984) *J. Am. Chem. Soc. 106*, 1139.

Smith, M. L., Ohlsson, P.-I., & Paul, K.-G. (1983) *FEBS Lett. 163*, 303.

Smulevich, G., Evangelista-Kirkup, R., English, A., & Spiro, T. G. (1986) *Biochemistry 25*, 4426.

Smulevich, G., Mauro, J. M., Fishel, L. A., English, A. M., Kraut, J., & Spiro, T. G. (1988) *Biochemistry* (preceding paper in this issue).

Stein, P., Mitchell, M., & Spiro, T. G. (1980) *J. Am. Chem. Soc. 102*, 7795.

Takano, T. (1977) *J. Mol. Biol. 110*, 537.

Teraoka, J., & Kitagawa, T. (1981) *J. Biol. Chem. 256*, 3969.

Tsubaki, M., Srivastava, R. V., & Yu, N.-T. (1982) *Biochemistry 21*, 1132.

Uno, T., Nishimura, Y., Tsuboi, M., Makino, R., Iizuka, T., & Ishimura, Y. (1987) *J. Biol. Chem. 262*, 4549.

Walters, M., & Spiro, T. G. (1982) *Biochemistry 21*, 6989.